VERTICAL DENSITY PROFILE AND INTERNAL BOND STRENGTH OF WET-FORMED PARTICLEBOARD BONDED WITH CELLULOSE NANOFIBRILS

John F. Hunt

Research General Engineer
Email: jfhunt@fs.fed.us

*Weiqi Leng**†

Post-doctoral Research Associate
Engineered Composites Science
U.S. Department of Agriculture, Forest Service, Forest Products Laboratory
Madison, WI 53726
E-mail: wleng@fs.fed.us

*Mehdi Tajvidi**†

Assistant Professor
School of Forest Resources
University of Maine Orono, ME 04469
E-mail: mehdi.tajvidi@maine.edu

(Received March 2017)

Abstract. In this study, the effects of cellulose nanofibrils (CNFs) ratio, press program, particle size, and density on the vertical density profile (VDP) and internal bond (IB) strength of the wet-formed particleboard were investigated. Results revealed that the VDP was significantly influenced by the press program. Pressing using a constant pressure (CP) press program produced panels with flat-shaped profile. Panels made from a constant thickness (CT) press program produced U-shaped profile. The CNF ratio and density also influenced the VDP especially for the CT panels. As the CNF ratio increased, there were noticeable increases in face density, while the core density slowly increased. The CT panels had the lowest core density compared with the CP counterparts, thus significantly lowering the IB. The IB of CP panels increased with the increase of CNF ratio, but the trend for CT panels was different. For the 10% CNF ratio, the IB increased as the core density increased. For the 15% and 20% CNF ratios, the IB decreased as the core density increased. For CP panels, the minimum core densities were higher and thus the IB was significantly higher. None of the panels met the IB values for high-density standard particleboard. All CP panels met some of the medium-density standard IB values and all the low-density standard IB values. However, for the CT panels, only those with 15% and 20% CNF ratio marginally met the low- and medium-density particleboard standard. Trends show that increased CNF ratio and higher pressure could improve IB properties for the high-density particleboard.

Keywords: fractional factorial design, vertical density profile, internal bond, CNF ratio, pressing method, core and face density.

INTRODUCTION

Vertical density profile (VDP) is an important parameter that relates to both mechanical and physical properties of particleboard. VDP shows the density variation through the thickness direction (Wang et al 2001; Nemli and Demirel 2007), which starts to develop when the top and bottom hot-press platens contact the surface of the wet mat. The mat undergoes change as internal steam pressure, MC, and thickness interact during the drying process (Wang et al 2000; Wang and Winistorferf 2000; Winistorfer et al 2000). VDP can be affected by a number of factors, such as raw material properties, mat

* Corresponding author
† SWST member

© 2016 by the Society of Wood Science and Technology

properties, hot-press parameters (Kelly 1977; Suchsland and Woodson 1986; Nemli and Demirel 2007).

There are two different types of VDP named as U-shaped and flat-shaped density profiles (Wong et al 1999). During the hot-pressing process, the interaction between heat and moisture facilitates the plasticization of wood particles, and forms denser face regions (Gamage et al 2009). The moisture will turn into steam, part of which moves out of the mat system, whereas the rest moves toward the core region of the mat and heats up the region. The density in the core region normally is lower than that in the face region, which results in the U-shaped density profile (Gamage et al 2009); however, the press parameters can be manipulated to generate a higher density in the core region, which forms the flat-shaped density profile.

Internal bond (IB) strength is correlated to the VDP. For panels with U-shaped density profile, the core region is less dense resulting in lower IB strengths (Liiri et al 1980). However, some studies have shown that it was the mean density, not the VDP, which had a higher correlation to the IB strength (Schulte and Fruhwald 1996). The panel morphology, defects inside the panel, and hot-pressing affects the IB strength as well. IB can be improved by reducing the particle size due to the increased surface area (Li et al 2010). During hot-pressing, the steam pressure facilitates the heat conduction from the mat surface into the core area and the plasticization of wood particles (Biswas et al 2011). Higher pressure results in better IB strength (Buyuksari et al 2010). In addition, high compaction ratio of particleboard mats generates faster heat transfer to the core area and results in higher IB strength (Tabarsa et al 2011).

Cellulose nanofibrils (CNF) is defined as the defibrillated cellulose fibers with a width in the nanometer grade (Zhang et al 2013). Mechanically derived CNF is made by repeated refining and a large pressure drop with shearing and impact forces, and chemical pretreatment is preferred to save the energy cost (Nakagaito and Yano 2004). The CNF is a great candidate to produce binderless particleboard due to its strong mechanical properties and web-like network that can improve the interfacial adhesion (Shao et al 2015). However, only a few researchers have investigated the production of binderless boards (Baskaran et al 2012; Hashim et al 2012; Boon et al 2013; Arévalo and Peijs 2016; Euring et al 2016; Tajvidi et al 2016). In this study, wet-formed particleboard panels were produced using CNF as the only bonding agent. The effect of different press programs, CNF ratio, and the properties of the wood particles were investigated on the development of VDP and IB strength.

MATERIALS AND METHODS

Fabrication of CNF-Bonded Particleboard

Materials: wood particles, CNF. The wood particles used in this study consisted of a 80:20 ratio of softwood:hardwood. The MC was 6.8%. To help characterize the wood particles, they were screened through a 1.59-and a 0.79-mm opening vibrating sieve to obtain three fractions. The fractions were then collected and weight percentages determined, as shown in Table 1. Bulk T1 density for each fraction was also determined. Analysis of the particle fractions was determined using image analysis to determine an estimated surface area. The particles were obtained from the original mixture of particles and were spread out on a white piece of paper sheet. Photos were then taken via a digital camera. Fiji image analysis software (LOCI, 1st version, Madison, WI) was used to estimate the major length vs minor length. The assumption was that these dimensions could be used to estimate a cylinder length and diameter, respectively. Surface could then be estimated using cylinder surface equations. Mechanically

Table 1. Wood particle characterization.

Wood particle	Particle size > 1.59 mm opening	Particle size 1.59 mm > opening > 0.79 mm	Particle size < 0.79 mm opening
Weight percentage	17.74	41.52	40.74
Bulk density (kg/m^3)	168	202	226
Surface area (m^2/g)	Not applicable	0.2	8.08

derived CNF with a solids content of 3% was provided by the process development center at University of Maine (Orono, ME). The average dimension of the CNF was around 300 nm, with the length of several micros.

Panel fabrication. In this study, particleboard panels with the final dimensions of 305 × 305 × 12.7 mm were fabricated. The fractional factorial experiment design was used, as shown in Table 2. The effects of press program types, CNF ratio, target density, and particle size on panel VDP and IB strength were investigated. Three replicates of each treatment were produced. Wood particles and CNF were mixed uniformly with a Hobart laboratory blender (The Hobart MFG, Co., Troy, OH). The mixture was blended for 15 min. The CNF was uniformly distributed throughout the mixture. Then the mixture was evenly distributed in a 305-mm square forming box. A flat plate was placed on top of the distributed mixture and approximately 65-75 N/m^2 vacuum pressure was used to precompress the semiwet mat and to remove a portion of the free water. The precompressed mats were then transferred onto a screen on top of an aluminum caul. A 305-mm^2 aluminum frame was carefully placed around the mat to prevent the mat from extruding sideways during hot-pressing. A second screen was placed between the top of the mat, and two 25.4-mm-thick aluminum plates were placed inside the frame and on top of the wet mat. The total package was placed into a hot-press (Williams White Co., Moline, IL). The platens were steam heated and set at 185°C. Constant pressure (CP) and constant thickness (CT) press programs were evaluated for the drying process, as shown in Table 2. Typical CT and CP schedules are shown in Fig 2. High pressure occurred initially as the wet mat was consolidated and dewatered as the heat transferred into the mat. For all of the panels, the excess water was pressed out of the mixture as the press closed on the CNF/particle mixture. The panels were pressed to near oven-dry conditions before the panels were removed. Prior to testing, the finished panels were cut according the standard test dimensions where possible and then were conditioned in a 20°C and 65% RH conditioning room for 4 wk.

Table 2. Experiment design.

ID	Particle size	CNF ratio (%)	Target density (kg/m^3)	Pressure type
1	L	10	600	CT
2	L	10	750	CP 0.41 MPa
3	L	10	900	CP 0.55 MPa
4	L	15	600	CP 0.41 MPa
5	L	15	750	CP 0.55 MPa
6	L	15	900	CT
7	L	20	600	CP 0.55 MPa
8	L	20	750	CT
9	L	20	900	CP 0.41 MPa
10	F	10	600	CP 0.41 MPa
11	F	10	750	CP 0.55 MPa
12	F	10	900	CT
13	F	15	600	CP 0.55 MPa
14	F	15	750	CT
15	F	15	900	CP 0.41 MPa
16	F	20	600	CT
17	F	20	750	CP 0.41 MPa
18	F	20	900	CP 0.55 MPa
19	M	10	600	CP 0.55 MPa
20	M	10	750	CT
21	M	10	900	CP 0.41 MPa
22	M	15	600	CT
23	M	15	750	CP 0.41 MPa
24	M	15	900	CP 0.55 MPa
25	M	20	600	CP 0.41 MPa
26	M	20	750	CP 0.55 MPa
27	M	20	900	CT

L, large size particles; F, fine size particles; M, mixed size particles; CP, constant pressure; CT, constant thickness; CNF, cellulose nanofibrils.

Characterization

Determination of VDP. The VDP was determined in the QDP-01X system (QMS Inc. Knoxville, TN). Six specimens with the size of nominally 50 × 50 mm were inserted into the cassette holder for each batch scan. During scanning, the density was recorded every 0.05 mm. Data were analyzed and the VDP was determined by the Origin software (OriginLab Corporation, Northampton, MA). The same specimens were used for the IB test after the scan of VDP.

IB test. The IB strength was determined according to standard American Society for Testing and Materials (ASTM) D1037-12 (2012). The same specimens used for the VDP scan were bonded to 50 × 50 mm steel blocks using hot melt adhesive.

The test was conducted on the 50 kN Instron machine (Norwood, MA). Continuous uniform load was applied until failure of the specimen. The rate of motion of the crosshead was set to 1.02 mm/min. SAS software (SAS Institute Inc., Cary, NC) was applied to analyze the effect of each parameter on the IB property. The data were analyzed using analysis of variance (ANOVA).

RESULTS AND DISCUSSIONS

The Effect of Press Program and Particle Size on VDP

F1 Figure 1a-c shows typical VDP shapes. All low-density (600 kg/m^3) target panels manufactured via CP press program demonstrated a relatively flat-shaped density profile, as shown Fig 1c. Figure 1a shows typical shape for both medium- and high-target density (750 and 900 kg/m^3) panels manufactured via the CP press program. The outer faces exhibited specific higher peak density regions while generally flatter in the core. However, those made with CT press program had a pronounced U-shaped profile, as shown in Fig 1b. Figure 2 shows the displacement and pressure F2 variations during the both CT and CP press process. For the CT press program, the pressure decreased exponentially to near zero after reaching the target thickness. The particles and CNF in the face region were softened by steam

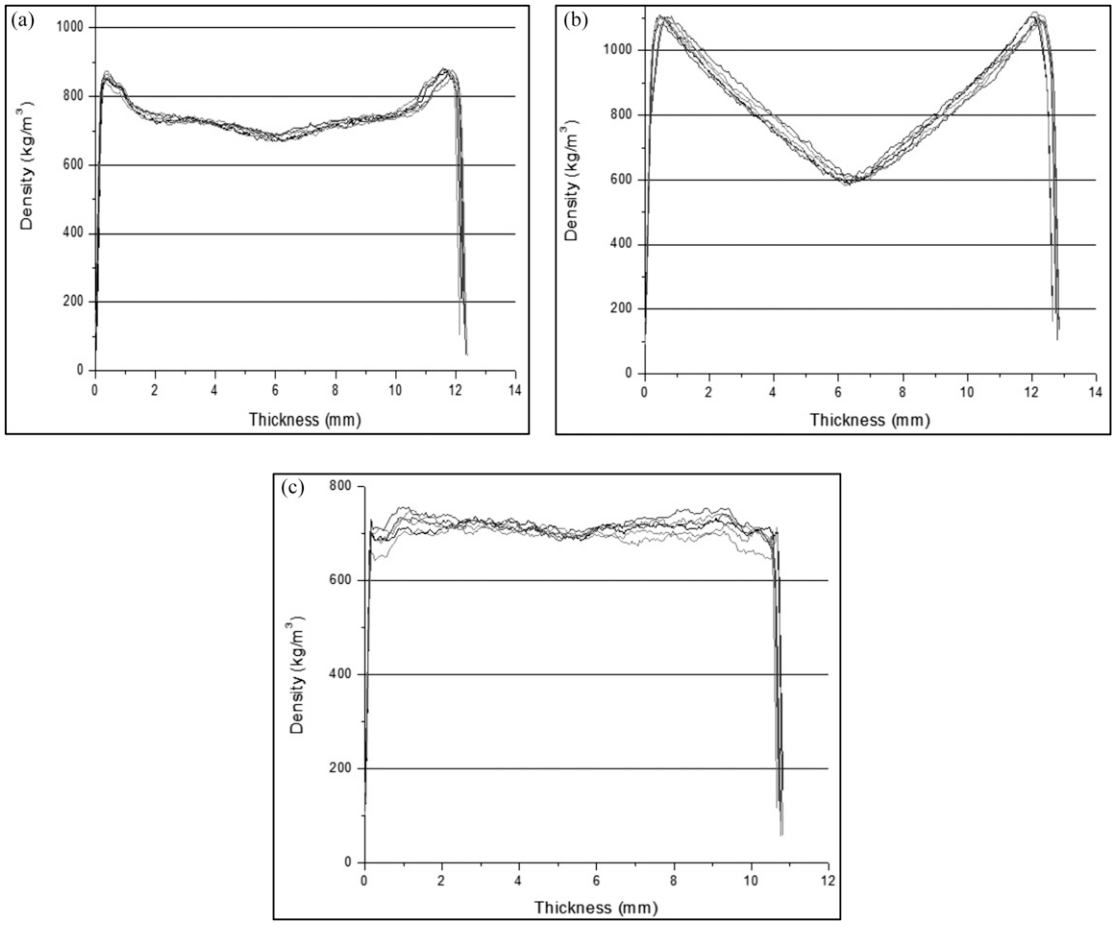

Figure 1. The general vertical density profile shape of panels manufactured with (a) constant pressure (CP) press program for medium- and high-target density panels (750 and 900 kg/m^3); (b) all constant thickness (CT) press program; and (c) CP press program for low-target density (600 kg/m^3).

and densified more by the pressure. Pressure decreased while thickness was held constant as moisture left, resulting in decreasing pressure in the core as the moisture left and decreasing board density with lowering pressure, as shown in Fig 2. Hence the core region density decreased as a function of pressure compared with the face region. Whereas, the CP press program showed that the pressure remained constant until the platen opened. It was relatively easy to determine

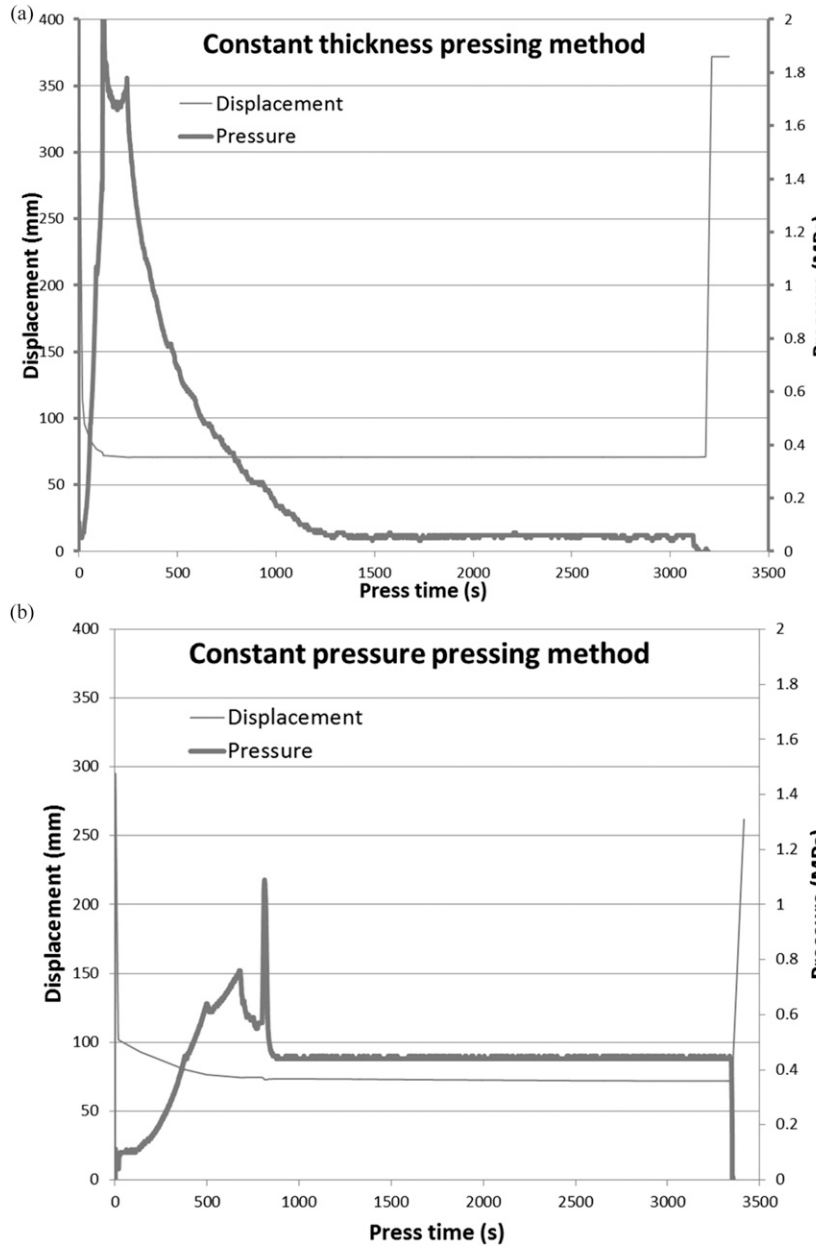

Figure 2. The displacement and pressure variation graph for panels made with (a) CT press program and (b) CP press program.

when the board was dry with CP process, which was the point when the mat thickness stopped decreasing. Under CP press program, decreasing mat thickness indicated moisture loss during the drying process. In the face region, higher density developed initially as the combined effects of temperature, pressure, and steam to consolidate the wood particles and CNF as moisture easily passed through the face surface, which was the same mechanism for the CT press program. In the core region, the CP provided by the platens enabled the wood particles to be continually densified, thus higher core density was achieved.

For panels manufactured with CP press program, the VDP for all low target density (600 kg/m^3) panels (Fig 1c) exhibited nearly flat density profiles as compared with those of medium (750 kg/m^3) and high (900 kg/m^3) target densities ones, as shown in Fig 1a. Before hot-pressing, the initial mat thickness for the low target density panels was thinner than the medium- or high-density panels. The time duration for the top platen to contact the top surface of the mat was longer and may have impacted the surface density characteristics.

It is well known that most failures occur in the low-density core region during the IB test (Xu et al 2005). However, in this study, the failure mode for many low-target density (600 kg/m^3) panels hot-pressed through CP press program was slightly different. Many specimens failed close to the surface of either face, while some failed in the core region, where the density was slightly higher than the face region, as shown in Fig 1c, where the density in either of the faces gradually increases to the mean density in the rest of the panel.

For density analysis, the board was divided into three 1/3 sections. Figure 3a-c shows lowest density value in the core for the middle 1/3 section of the panel and the mean densities of the faces in the outer 1/3 top and bottom sections of the panel. All density values either low or high are plotted against the mean density of that panel. There is a midline through each of the figures showing the 1:1 line for low or high density to the mean density. Figure 3a and b show that the lowest core densities for the CP press program either at 0.41 or 0.55 MPa. The lowest densities for both pressures did not deviate much from the mean panel density. The lowest density decreased from the mean density only slightly as the mean density increased. The effect of CNF ratio on lowest density core regions was not obvious as the mean density increased. However, as the mean density increased the highest face densities increased remarkably. The highest face densities also increased with higher CNF ratio especially for those with higher press pressures, as shown in Fig 3b. The CP process provided a method that rendered the panel a more uniform density profile. Whereas, the CT press program, Fig 3c, as used in this study exhibited a larger difference between the lowest core densities and the high face densities. This is characteristic of CT pressing program. It is also interesting to note that the lowest core density for all CT panels exhibited similar trends for the low-density values as the mean density increased. However, the highest face density increased with increasing mean density and increased based on increased CNF ratio.

The Effect of Press Program, CNF ratio, Particle Size, and Target Density on the IB Strength

The ANOVA table (Table 3) shows that all four factors were significantly important on the IB strength of the panels, of which the CNF ratio and the types of press program were the most important, followed by target density and particle size. The IB was correlated to the VDP of particleboard. Figure 4 shows that panels manufactured with CP press program had higher IB values than those with CT press program, as expected due to the higher core density of the CP panels. Although the mean density was the same, the core region of the panels manufactured with CT press program had lower density, which resulted in a weaker core region. The IB results also demonstrated that higher press pressure produced higher IB for panels manufactured with CP press program. The IB strength consisted of

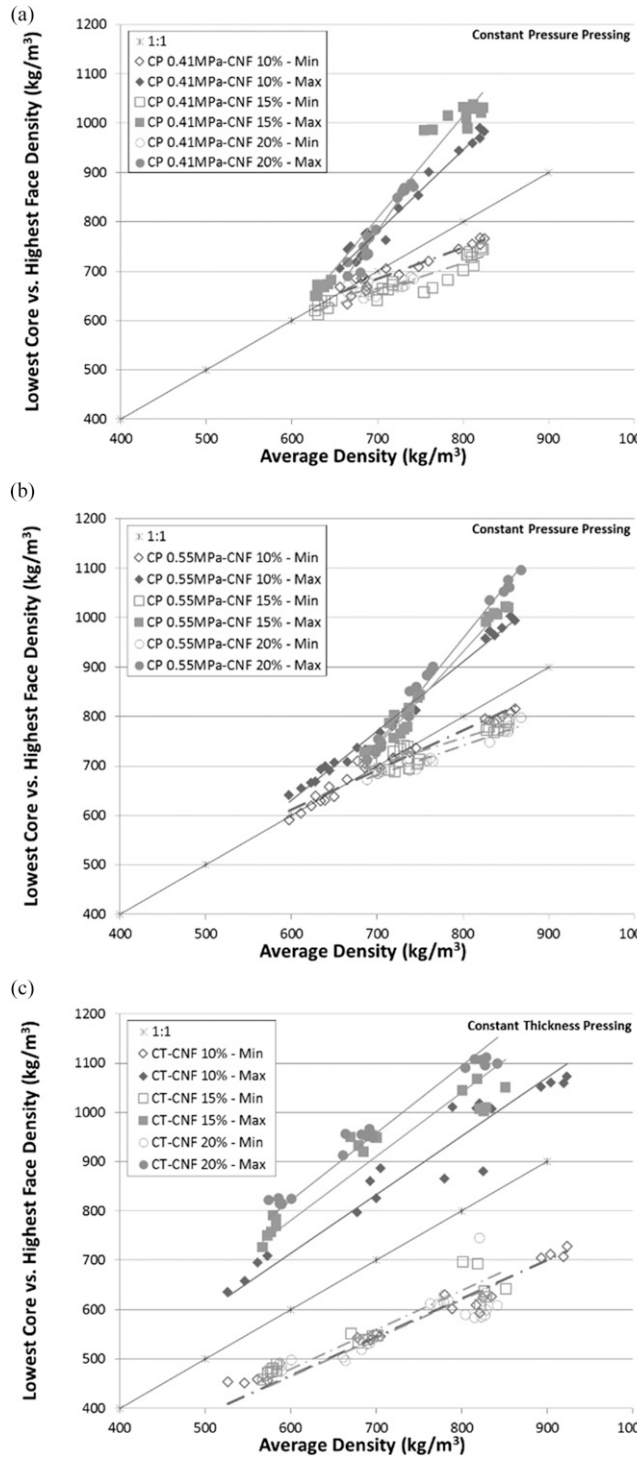

Figure 3. Plot of lowest core densities vs highest face densities for (a) CP pressing 0.41 MPa; (b) CP pressing 0.55 MPa; and (c) CT pressing.

Table 3. Analysis of variance table for internal bond.

Source	F	p value
Particle size	130.8776	<0.0001
CNF ratio	487.5814	<0.0001
Density	140.5796	<0.0001
Pressure type	282.9526	<0.0001
Particle size × CNF ratio	13.28686	<0.0001
Particle size × Density	18.55682	<0.0001
Particle size × Pressure type	12.55627	<0.0001
CNF ratio × density	0.097621	0.7558
CNF ratio × pressure type	0.132197	0.8764
Density × pressure type	31.54582	<0.0001

CNF, cellulose nanofibrils.

two sources, the bonding within wood particles and that between wood particles and CNF (Leng et al 2017). Higher hot-press pressures made wood particles more compressed, which increased the contact area between wood particles and CNF and also within wood particles, and also increased the possibility of hydrogen bonding between particles and CNF, thus obtaining higher bonding strength (Boon et al 2013).

CNF ratio played a dominant role for the IBs especially for the CP panels. Higher CNF ratio indicated increased bonding sites between CNF and wood particles. Moreover, extra CNF could fill the voids and agglomerate, providing additional bonding strength under compressive pressure and reducing defects within the panel. Similar statement was reported by Arévalo and Peijs (2016). For the CT panels with 10% CNF ratio, the IB values increased with increasing density, while for those made with 15% and 20% CNF ratios, the IBs gradually decreased as the density increased. We are not sure why at this point but it is possible that the panels were not dried fully before the press was opened. As we mentioned earlier, it was more difficult to determine the oven-dry point of the panels made with the CT press program. It is possible that with the extra moisture that was attributed to the higher CNF ratio, the press was opened prematurely causing steam to expand within the panel, which was sufficient to disrupt some of the interfiber bonding. Further testing isneeded to determine if the panels were dried enough for panels with higher CNF ratio.

The effect of particle size on the IB was the least significant, and there were significant interactive effects between particle size and other variables, as shown in Table 3. The panels manufactured with fine particles had the strongest IB when the preselected CNF ratio and target density were the highest, which is probably due to higher surface area resulted from fine particles (Quintana et al 2009). The surface morphology was also more uniform with finer particles. For panels manufactured with mixed size particles and hot-pressed at 0.55 MPa CP, the target density was more important than the CNF ratio on IB values. The reason was that fine particles could fill the voids made by large particles, easily filling between wood particles and CNF. Panels made with larger particles had poor bonding performance. It is possible that small voids were formed due to the larger particle size geometry, resulting in less contact area between wood particles and CNF (Suchsland et al 1985; Arabi et al 2011). Again, these defects can be minimized by adding more CNF, which would increase the number of bonding sites, and decrease the bonding discontinuity.

For all panels manufactured with CT press program, the density profile was U shaped with low core density, and the IB tests confirmed that all specimens broke in the core region. As shown in Fig 4c, all panels pressed with the CP press method either met all low-density standard requirements and some of the medium-density standard requirements according to American National Standards Institute (ANSI) A208.1-2016 (2016). It is possible that increased CNF ratio would have increased the IB values to meet the medium density, even high-density standard requirements. However, panels made with CT press method were only able to meet the low-density IB standard requirements. Similar results were reported in other studies (Boon et al 2013; Nair et al 2013). As mentioned earlier, it is possible the panels were not sufficiently dry and premature failure occurred with the higher CNF ratios upon press opening. This would be consistent with the slight downward trend of the

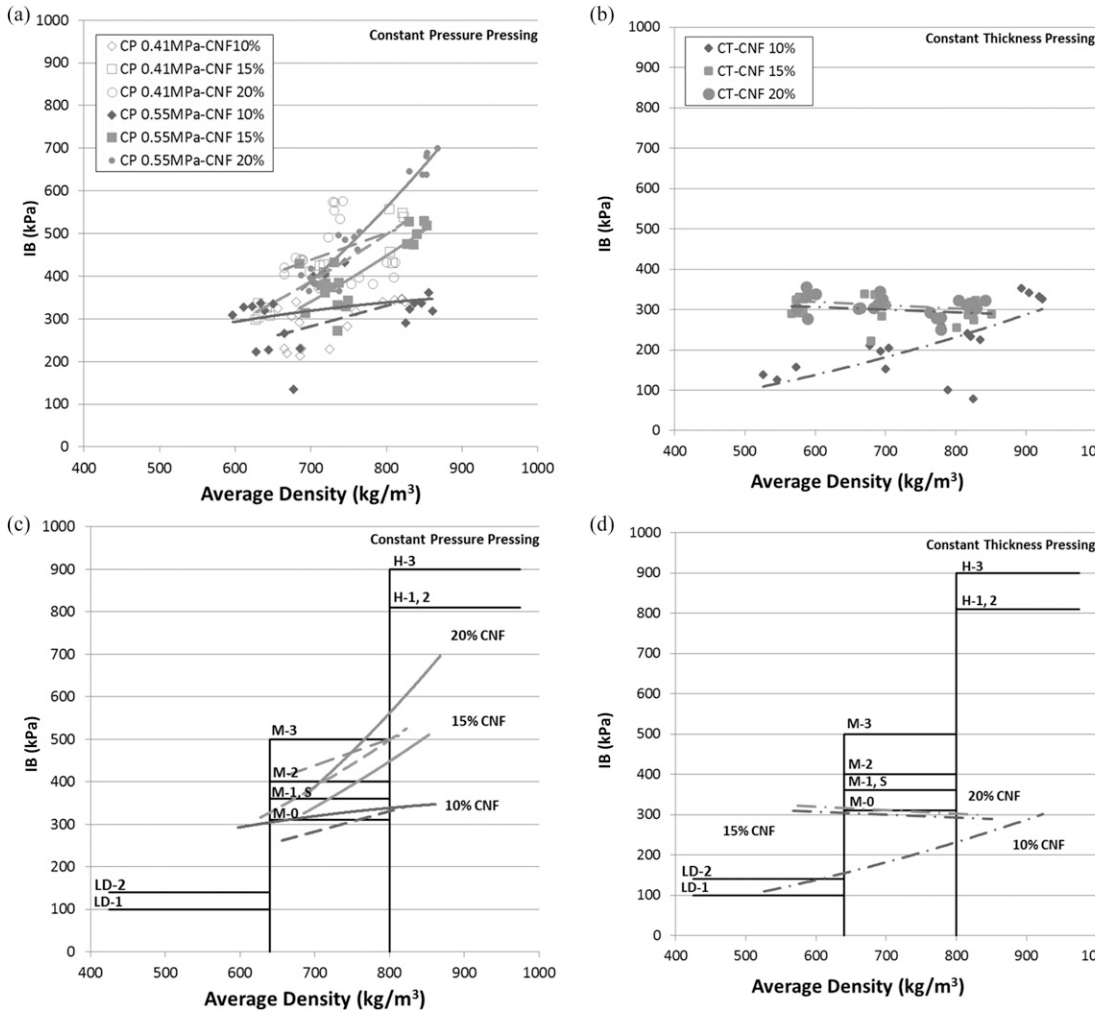

Figure 4. IB values for (a) CP press program data for 0.41 and 0.55 MPa at 10%, 15%, and 20% CNF; (b) CT press program at 10%, 15%, and 20% CNF; (c) CP press program IB trends compared with minimum IB standards; and (d) CT press program IB trends compared with minimum IB standards.

IB values for panels with 15% and 20% CNF ratio.

CONCLUSIONS

The shape of VDP was dependent on the types of press program, with a flat-shaped profile for panels made with CP press program, and a U-shaped profile for those made with CT press program. At all CNF ratios, the density profile was essentially flat up to 650 kg/m^3 at 0.41 MPa and 700 kg/m^3 at 0.55 MPa. As density increased, the highest face densities increased with a slightly decreased dip in the core. This would correlate with increased CNF ratio, more moisture in the panel, and a tighter pathway for steam to escape. The press program also had a significant effect on the IB values. CP press program resulted in higher IBs than the CT press program, given the other parameters the same. Panels made with CT press program had lowest core density while exhibiting an increasing face density as the mean density and CNF ratio increased. The lowest core

density increased as the mean density increased for all CNF ratios, but IB values for panels with 15% and 20% CNF ratios did not follow the same trends. More analysis needs to be done with the CT press program to determine entrained steam as the panel dries.

All CP panels either met low- and medium-density ANSI standard IB requirements and trends indicated that it was possible to meet high density standard requirements at higher panel densities or CNF ratio or both. CT panels were only able to meet low-density ANSI standard requirements and the lowest medium density standard requirements at the 20% CNF ratio. It is possible the panels showed signs of premature failure due to increased steam pressure when the press opened at the end of the cycle. More work is needed to validate this assumption and to determine how CT press program could be used with the increase of CNF ratio to meet basic standard requirements.

ACKNOWLEDGMENTS

We would like to acknowledge Sara Fishwild, Timothy Nelson, Marshall Begel, James Bridwell, J. for their help with the property test, and Patricia K. Lebow for her help with the statistical analysis. This study was funded by the P3Nano project No. P3-5.

REFERENCES

American National Standards Institute (ANSI) (2016) American national standard for particleboard. a208.1-2016. Composite Panel Association, Leesburg, VA.

American Society for Testing and Materials (ASTM) (2012) Standard test methods for evaluating properties of wood-base fiber and particle panel materials. D 1037-12. American Society for Testing and Materials, West Conshohocken, PA.

Arabi M, Faezipour M, Layeghi M, Enayati AA (2011) Interaction analysis between slenderness ratio and resin content on mechanical properties of particleboard. *J For Res* 22:461-464.

Arévalo R, Peijs T (2016) Binderless all-cellulose fiberboard from microfibrillated lignocellulosic natural fibres. Compos Part A 83:38-46.

Baskaran M, Hashim R, Said N, Raffiet alBalakrishnan K, Sudesh K, Sulaiman O, Arai T, Kosugic A, MoricY (2012) Properties of binderless particleboard from oil palm trunk with addition of polyhydroxyalkanoates. Compos, Part B Eng 43:1109-1116.

Biswas D, Kanti Bose S, Mozaffar Hossain M (2011) Physical and mechanical properties of urea formaldehyde-bonded particleboard made from bamboo waste. Int J Adhes Adhes 31:84-87.

Boon JG, Hashim R, Sulaiman O, Sato M (2013) Influence of processing parameters on some properties of oil palm trunk binderless particleboard. Eur J Wood Wood Prod 71: 583-589.

Buyuksari U, Ayrilmis N, Avci E, Koc E (2010) Evaluation of the physical, mechanical properties and formaldehyde emission of particleboard manufactured from waste stone pine (*Pinus pinea* L.) cones. Biores Technol 101: 255-259.

Euring M, Kirsch A, Schneider P, Kharazipour A (2016) Lignin-Laccase-Mediator-Systems (LLMS) for the production of binderless medium density fiberboards (MDF). J Mater Sci Res 5:7.

Gamage N, Setunge S, Jollands M, Hague J (2009) Properties of hardwood saw mill residue-based particleboards as affected by processing parameters. Ind Crops Prod 29: 248-254.

Hashim R, Nadhari WNAW, Sulaiman O, Sato M, Hiziroglu S, Kawamura F, Sugimoto T, Seng TG, Tanaa R (2012) Properties of binderless particleboard panels manufactured from oil palm biomass. BioResources 7: 1352-1365.

Kelly MW (1977) Critical literature review of relationship between processing parameters and physical properties of particleboard. USDA Forest Serv., Forest Prod. Lab., Madison, WI.

Leng W, Hunt JF, Tajvidi M (2017) Effects of density, cellulose nanofibrils addition ratio, pressing method, and particle size on the bending properties of wet-formed particleboard. *BioResources* 12:4986-5000.

Li X, Cai Z, Winandy JE, Basta AH (2010) Selected properties of particleboard panels manufactured from rice straws of different geometries. Biores Technol 101:4662-4666.

Liiri O, Kivistoe A, Tuominen M, Aho M (1980) Determination of the internal bond of particleboard and fibreboard. Holz Als Roh- Werkst 38:185-193.

Nair M, Gupta A, Beg MDH, Chua GK, Jawaid M, Kumar A, Khan TA (2013) Fabricating eco-friendly binderless fiberboard from laccase-treated rubber wood fiber. BioResources 8:3599-3608.

Nakagaito AN, Yano H (2004) The effect of morphological changes from pulp fiber towards nano-scale fibrillated cellulose on the mechanical properties of high-strength plant fiber based composites. Appl Phys Mater Sci Process 78:547-552.

Nemli G, Demirel S (2007) Relationship between the density profile and the technological properties of the particleboard composite. J Compos Mater 41:1793-1802

Quintana G, Velasquez J, Betancourt S, Ganan P (2009) Binderless fiberboard from steam exploded banana bunch. Ind Crops Prod 29:60-66.

Schulte M, Fruhwald A (1996) Some investigations concerning density profile, internal bond and relating failure position of particleboard. Holz Als Roh- Werkst 54: 289-294.

Shao Y, Yashiro T, Okubo K, Fujii T (2015) Effect of cellulose nano fiber (CNF) on fatigue performance of carbon fiber fabric composites. Compos Part Appl Sci Manuf 76:244-254.

Suchsland O, Woodson GE (1986) Fiberboard manufacturing practices in the United States. USDA Forest Service, Madison, WI. pp. 112-158.

Suchsland O, Woodson GE, Mcmillin CW (1985) Binderless fiberboard from two different types of fiber furnishes. For Prod J 35:63-68.

Tabarsa T, Ashori A, Gholamzadeh M (2011) Evaluation of surface roughness and mechanical properties of particleboard panels made from bagasse. Compos, Part B Eng 42: 1330-1335.

Tajvidi M, Gardner DJ, Bousfield DW (2016) Cellulose nanomaterials as binders: Laminate and particulate systems. J Renew Mater 4:365-376.

Wang S, Winistorfer PM, Young TM (2000) Fundamentals of vertical density profile formation in wood composites. Part III. MDF density formation during hot-pressing. Wood Fiber Sci 36:17-25.

Wang S, Winistorfer PM, Young TM, Helton C (2001) Step-closing pressing of medium density fiberboard; Part 1. Influences on the vertical density profile. Eur J Wood Wood Prod 59:19-26.

Wang S, Winistorferf PM (2000) Fundamentals of vertical density profile formation in wood composites. Part II. Methodology of vertical density formation under dynamic conditions. Wood Fiber Sci 32:220-238.

Winistorfer PM, Moschler WW, Wang S, DePaula E, Bledsoe BL (2000) Fundamentals of vertical density profile formation in wood composites. Part I. In-situ density measurement of the consolidation process. Wood Fiber Sci 32:209-219.

Wong E-D, Zhang M, Wang Q, Kawai S (1999) Formation of the density profile and its effects on the properties of particleboard. Wood Sci Technol 33:327-340.

Xu J, Widyorini R, Kawai S (2005) Properties of kenaf core binderless particleboard reinforced with kenaf bast fiber-woven sheets. J Wood Sci 51:415-420.

Zhang Y, Nypelö T, Salas C, Arboleda J, Hoeger IC, Rojas OJ (2013) Cellulose nanofibrils: From strong materials to bioactive surfaces. J Renew Mater 1:195-211.